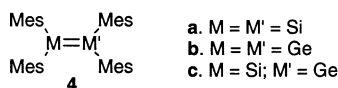
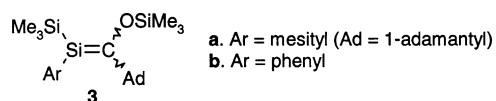
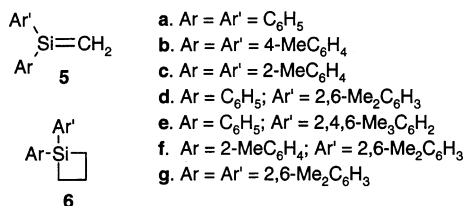




stabilization of reactive molecules, and the situation is similar in the literature for metallaenes and dimetallaenes. For example, silene **1b** was one of the first silenes to be isolated and characterized;<sup>3</sup> the first (and evidently the only) stable silene bearing a mesityl substituent at silicon (**3a**) was reported sometime later.<sup>7</sup> The latter silene can be compared to the phenyl derivative **3b**, which was found to dimerize to the corresponding 1,2-disilacyclobutane under the reaction conditions employed to prepare it.<sup>8</sup> In the dimetallaene literature, the tetramesityl compounds **4a–c** include the first disilene<sup>9</sup> and germsilene<sup>10</sup> derivatives to be isolated and characterized in the solid state. The reactivities of these compounds have been extensively investigated; indeed, almost all of the kinetic and/or mechanistic work that has been reported to date on dimetallaene reactions in solution has been carried out with these or other sterically stabilized derivatives. The opposite situation is found in the literature on silenes and germenenes, where the bulk of the mechanistic work that has been reported has been carried out with transient M=C derivatives.<sup>1</sup> The effects of sterically stabilizing substituents on the mechanisms of metallaene and dimetallaene reactions are not known, or at best not well understood.



In this paper, we report the results of a systematic study of the effects of *ortho*-methyl substitution on the kinetics and mechanisms of several characteristic reactions of 1,1-diarylsilenes, of which 1,1-diphenylsilene (**5a**) is the parent congener. Five different silenes (**5c–g**) have been studied, all by the technique of laser flash photolysis, using the corresponding 1,1-diarylsilacyclobutanes (**6c–g**) as the silene precursors. Coupled with the results of some of our previous studies on the effects of *para* ring substituents on the reactivity of **5a**,<sup>11</sup> in particular those for 1,1-bis(4-methylphenyl)silene (**5b**), the present results provide a quantitative assessment of both the electronic and steric effects of *ortho*-methyl substitution on 1,1-diarylsilene reactivity.

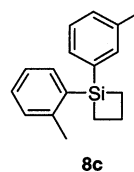
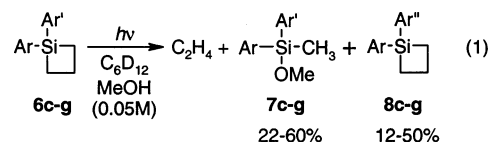


## Results

The 1,1-diarylsilacyclobutanes **6c–g** were prepared in 40–90% overall yield by addition of the appropriate

aryl Grignard reagent(s) to 1,1-dichlorosilacyclobutane, either in one step (**6c** and **6g**) or two (**6d–f**), with the more hindered aryl group being added first.<sup>12</sup>

Steady state photolysis of argon-saturated 0.05 M solutions of **6c–g** in cyclohexane-*d*<sub>12</sub> containing methanol (0.05 M) led to the formation of ethylene, the 1,1-diarylmethoxymethylsilane (**7c–g**) expected from trapping of the corresponding silene by the alcohol, and an isomer of the starting material (**8c–g**) (eq 1; two isomeric products were formed in the case of **6f**). The identities of **7c–g** were established by <sup>1</sup>H NMR spectroscopy and GC/MS and by comparing the spectra and GC retention times to those of independently synthesized authentic compounds in the cases of **7c** and **7g**. The mass spectra of the isomeric products were very similar to those of the starting materials in each case and are tentatively identified as arene phototransposition products.<sup>13</sup> This assignment was verified in the case of the isomeric product obtained from photolysis of **6c**, which was rigorously identified as **8c** by GC co-injection with an authentic, independently prepared sample. No other products were formed in yields greater than ca. 5% in any case, as long as the conversion of **6** was kept below ca. 15% in order to avoid secondary photolysis of the initially formed products (i.e., **8c–g**). The yield of the isomeric product was lowest (ca. 12%), and that of **7** highest (ca. 60%), in the case of **6g**. In most other cases, **7** and **8** were formed in similar chemical yields (see Supporting Information).



Photolysis of **6c–g** in deoxygenated hexane in the absence of methanol produced mixtures of several products in each case. In no case was a single major product formed, although the same isomeric products as were formed in the photolyses in the presence of methanol (i.e., **8c–g**) could be clearly identified. No clear evidence for the formation of silene dimers could be obtained by GC/MS analysis of the product mixtures in any case.

Laser flash photolysis experiments were carried out with solutions of **6c–g** (ca. 0.002 M) in dry acetonitrile

(6) Morkin, T. L.; Leigh, W. J.; Tidwell, T. T.; Allen, A. D. *Organometallics* **2001**, *20*, 5707.

(7) Brook, A. G.; Baumegger, A.; Lough, A. J. *Organometallics* **1992**, *11*, 3088.

(8) Baines, K. M.; Brook, A. G.; Ford, R. R.; Lickiss, P. D.; Saxena, A. K.; Chatterton, W. J.; Sawyer, J. F.; Behnam, B. A. *Organometallics* **1989**, *8*, 693.

(9) West, R.; Fink, M.; Michl, J. *Science* **1981**, *214*, 1343.

(10) Baines, K. M.; Cooke, J. A. *Organometallics* **1992**, *11*, 3487.

(11) Bradaric, C. J.; Leigh, W. J. *Can. J. Chem.* **1997**, *75*, 1393.

(12) Auner, N.; Grobe, J. *J. Organomet. Chem.* **1980**, *188*, 25.

(13) Gilbert, A. In *CRC Handbook of Organic Photochemistry and Photobiology*; Horspool, W. M., Song, P.-S., Eds.; CRC Press: New York, 1995; pp 229–236.

(2) Brook, A. G.; Nyburg, S. C.; Abdesaken, F.; Gutekunst, B.; Gutekunst, G.; Kallury, R. K. M. R.; Poon, Y. C.; Chang, Y. M.; Wong-Ng, W. *J. Am. Chem. Soc.* **1982**, *104*, 5667.

(3) Brook, A. G.; Wessely, H. J. *Organometallics* **1985**, *4*, 1487.

(4) Zhang, S.; Conlin, R. T.; McGarry, P. F.; Scaiano, J. C. *Organometallics* **1992**, *11*, 2317.

(5) Wiberg, N.; Wagner, G. *Angew. Chem., Int. Ed. Engl.* **1983**, *22*, 1005.

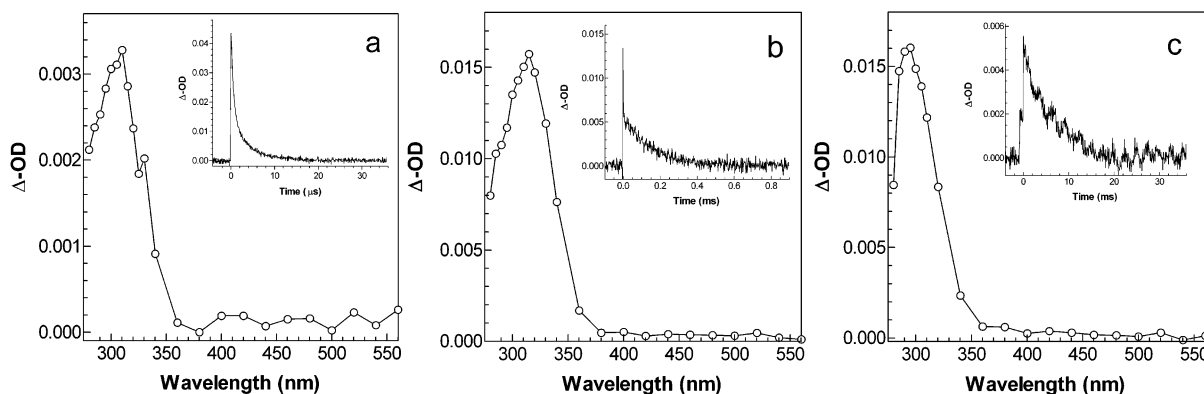


**Figure 1.** Transient absorption spectra of (a) 1,1-bis(2-methylphenyl)silene (**5c**), (b) 1-(2,6-dimethylphenyl)-1-phenylsilene (**5d**), and (c) 1,1-bis(2,6-dimethylphenyl)silene (**5g**) in acetonitrile solution at 25 °C. The spectra were recorded 4.9–9.0  $\mu\text{s}$  and 20–40  $\mu\text{s}$  (**5d**, **5g**) after laser excitation. The insets show typical transient absorption profiles, recorded at the absorption maxima. The short-lived components in the spectra of **5c** and **5d** exhibit absorption maxima of  $\lambda_{\text{max}} = 295$  and 297 nm, respectively, and lifetimes  $\tau \approx 1 \mu\text{s}$ .

**Table 1.** UV Absorption Maxima and Lifetimes of Silenes **5b–g** from Photolysis of 1,1-Diarylsilacyclobutanes **6b–g** in Dry, Deoxygenated Acetonitrile and Hexane Solution at 25 °C<sup>a</sup>

Ar(Ar')Si=CH <sub>2</sub>	Ar	Ar'	$\lambda_{\text{max}}/\text{nm}$	$\tau^{\text{MeCN}}/\mu\text{s}$	$\tau^{\text{hexane}}/\mu\text{s}$
<b>5b</b> <sup>b</sup>	4-MeC <sub>6</sub> H <sub>4</sub>	4-MeC <sub>6</sub> H <sub>4</sub>	325	3	7
<b>5c</b>	2-MeC <sub>6</sub> H <sub>4</sub>	2-MeC <sub>6</sub> H <sub>4</sub>	320	8	51
<b>5d</b>	Ph	2,6-Me <sub>2</sub> C <sub>6</sub> H <sub>3</sub>	315	144	1900
<b>5e</b>	Ph	2,4,6-Me <sub>3</sub> C <sub>6</sub> H <sub>2</sub>	315	420	1950
<b>5f</b>	2-MeC <sub>6</sub> H <sub>4</sub>	2,6-Me <sub>2</sub> C <sub>6</sub> H <sub>3</sub>	310	650	2700
<b>5g</b>	2,6-Me <sub>2</sub> C <sub>6</sub> H <sub>3</sub>	2,6-Me <sub>2</sub> C <sub>6</sub> H <sub>3</sub>	295	6100	8300

<sup>a</sup> Errors in lifetimes are estimated to be  $\pm 10\%$ . <sup>b</sup> From ref 11.

and hexane solutions, using the pulses from a KrF excimer laser for excitation ( $\sim 25$  ns, 248 nm, 90–130 mJ). Laser photolysis of **6c–f** produced two distinct transient species with overlapping absorption spectra in the 280–330 nm spectral range. In each case, the shorter-lived transient decayed with first-order kinetics and exhibited an absorption maximum ( $\lambda_{\text{max}}$ ) between 295 and 302 nm and a lifetime ( $\tau \approx 1 \mu\text{s}$ ) that did not vary significantly with solvent or substituent. The longer-lived transients also appeared to decay with first-order kinetics, but they exhibited absorption maxima and lifetimes that varied significantly throughout the series, from  $\lambda_{\text{max}} = 320$  nm and  $\tau \approx 50 \mu\text{s}$  for **6c** to  $\lambda_{\text{max}} = 310$  nm and  $\tau \approx 2.7$  ms for **6f** in dry hexane solution at 25 °C. A single long-lived transient absorption ( $\lambda_{\text{max}} = 295$  nm;  $\tau \approx 8.3$  ms) was observed in the case of **6g**. Identical absorption maxima were observed for these species in acetonitrile solution, but their lifetimes were 2–6 times shorter than in hexane. In each case, the lifetime of the longer-lived species was shortened upon addition of methanol (MeOH), acetic acid (AcOH), or *n*-butylamine (*n*-BuNH<sub>2</sub>) to the solutions (vide infra), while that of the shorter-lived transient was unaffected. Neither species' lifetime was affected upon oxygenation or addition of up to 1 M chloroform or 0.5 M triethylamine to the solutions. We assign the long-lived transient absorptions to the silenes **5c–g** on the basis of this behavior. We are unable to assign the short-lived transient species formed in the photolyses of **6c–f**; however, the insensitivity of their lifetimes to oxygen, methanol, chloroform, or amines effectively rules out a triplet state, silene, silylene, silyl radical, or radical cation assignment.

Time-resolved UV absorption spectra of silenes **5c**, **5d**,

and **5g** (i.e., the long-lived transients from laser photolysis of **6c**, **6d**, and **6g** in hexane or acetonitrile), recorded in point-by-point fashion over time windows after the decay of the short-lived species was complete, are shown in Figure 1 along with representative transient decay profiles recorded at the absorption maxima. The absorption maxima and estimated lifetimes of **5c–g** in hexane and acetonitrile solution at 25 °C are listed in Table 1.

As mentioned above, addition of MeOH, AcOH, and *n*-BuNH<sub>2</sub> to the solutions of **6c–g** caused reductions in the lifetimes of the long-lived transients assigned to **5c–g**. Plots of the pseudo-first-order decay rate constants ( $k_{\text{decay}}$ ) versus concentration of added reagent were linear for the carboxylic acid and amine and were analyzed according to eq 2, where  $k_0$  is the decay rate constant in the absence of added reagent and  $k_Q$  is the bimolecular rate constant for reaction with the added reagent at concentration [Q]. Representative plots are shown in Figure 2 for the quenching of **5d** and **5f** by these two reagents. Quenching of **5d**, **5e**, and **5g** by acetic acid-*Od* was also examined, and afforded  $k_Q$  values identical to those for the protiated acid within experimental error.

$$k_{\text{decay}} = k_0 + k_Q[\text{Q}] \quad (2)$$

In the case of MeOH, plots of  $k_{\text{decay}}$  versus [MeOH] were linear only in the case of **5c**. The plots were nonlinear for the other four silenes, so were fit to the quadratic eq 3, where  $k_{\text{MeOH}}$  and  $k_{2\text{MeOH}}$  are overall second- and third-order rate constants for reaction of the silene with one and two molecules of the alcohol, respectively. Quenching by methanol-*Od* was less ef-

**Table 2. Absolute Rate Constants for Reaction of Silenes 5a–g with MeOH, AcOH, and n-BuNH<sub>2</sub> in Deoxygenated Acetonitrile Solution at 25 °C<sup>a</sup>**

silene	$k_{\text{MeOH}}/10^6 \text{ M}^{-1} \text{ s}^{-1}$	$k_{2\text{MeOH}}/10^6 \text{ M}^{-2} \text{ s}^{-1}$	$k_{\text{AcOH}}/10^6 \text{ M}^{-1} \text{ s}^{-1}$	$k_{\text{n-BuNH}_2}/10^6 \text{ M}^{-1} \text{ s}^{-1}$
<b>5a</b>	1500 ± 100 <sup>b</sup>	<i>c</i>	1500 ± 200 <sup>b</sup>	2810 ± 60 <sup>d</sup>
<b>5b</b>	1120 ± 60 ( $k_{\text{H}}/k_{\text{D}} = 1.9 \pm 0.1$ )	<i>c</i>	1410 ± 50 ( $k_{\text{H}}/k_{\text{D}} = 1.2 \pm 0.2$ )	
<b>5c</b>	210 ± 70 ( $k_{\text{H}}/k_{\text{D}} = 1.3 \pm 0.1$ ) <sup>e</sup>	<i>c</i>	1600 ± 700	4700 ± 1600
<b>5d</b>	0.75 ± 0.14 ( $k_{\text{H}}/k_{\text{D}} = 2.6 \pm 1.5$ )	21 ± 2 ( $k_{\text{H}}/k_{\text{D}} = 1.4 \pm 0.2$ )	49 ± 2 ( $k_{\text{H}}/k_{\text{D}} = 1.0 \pm 0.2$ )	280 ± 12
<b>5e</b>	0.47 ± 0.10 ( $k_{\text{H}}/k_{\text{D}} = 1.5 \pm 0.6$ )	30 ± 2 ( $k_{\text{H}}/k_{\text{D}} = 2.5 \pm 0.4$ )	53 ± 4 ( $k_{\text{H}}/k_{\text{D}} = 1.0 \pm 0.2$ )	220 ± 12
<b>5f</b>	0.45 ± 0.10 ( $k_{\text{H}}/k_{\text{D}} = 1.7 \pm 0.4$ )	5.1 ± 0.8 ( $k_{\text{H}}/k_{\text{D}} = 2.1 \pm 0.4$ )	41 ± 3	103 ± 6
<b>5g</b>	<0.02 <sup>f</sup>	0.172 ± 0.003 ( $k_{\text{H}}/k_{\text{D}} = 1.6 \pm 0.2$ )	4.4 ± 1.5 ( $k_{\text{H}}/k_{\text{D}} = 1.1 \pm 0.1$ )	11 ± 6

<sup>a</sup> From analysis of the dependence of  $k_{\text{decay}}$  on  $[\text{Q}]$  according to eq 2 or 3 (see text). <sup>b</sup> From ref 11. <sup>c</sup> Linear dependence of  $k_{\text{decay}}$  on  $[\text{Q}]$  over the concentration range studied. <sup>d</sup> From ref 14. <sup>e</sup> Calculated from the rate constants for reaction in dry hexane solution;  $k_{\text{MeOH}} = (5.1 \pm 0.2) \times 10^8 \text{ M}^{-1} \text{ s}^{-1}$ . <sup>f</sup> Linear dependence of  $k_{\text{decay}}$  on  $[\text{Q}]^2$ .

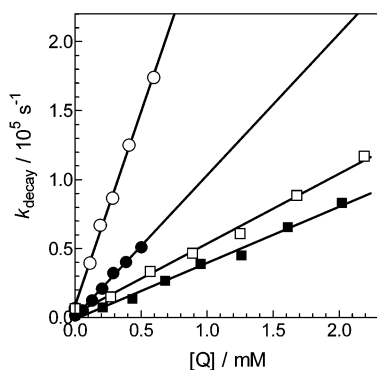


**Figure 2.** Plots of  $k_{\text{decay}}$  vs  $[\text{Q}]$  for quenching of 1-(2,6-dimethylphenyl)-1-phenylsilene (**5d**; circles) and 1-(2,6-dimethylphenyl)-1-(2-methylphenyl)silene (**5f**; squares) by *n*-butylamine (open symbols) and acetic acid (filled symbols) in acetonitrile solution at 25 °C.

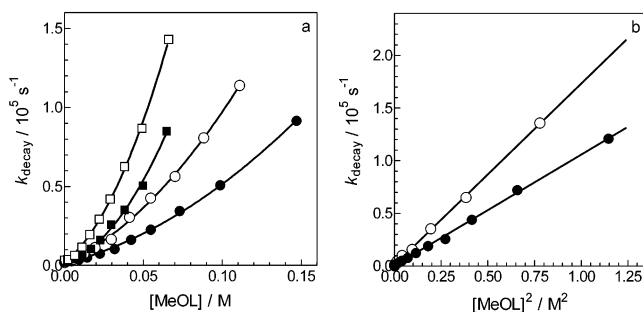


**Figure 3.** (a) Plots of  $k_{\text{decay}}$  vs  $[\text{MeOL}]$  for quenching of 1-(2,6-dimethylphenyl)-1-phenylsilene (**5d**; squares) and 1-(2,6-dimethylphenyl)-1-(2-methylphenyl)silene (**5f**; circles) by methanol (open symbols) and methanol-*Od* (filled symbols) in acetonitrile solution at 25 °C. (b) Plots of  $k_{\text{decay}}$  vs  $[\text{MeOL}]^2$  for quenching of 1,1-bis(2,6-dimethylphenyl)-1-phenylsilene (**5g**) by methanol (○) and methanol-*Od* (●) in acetonitrile solution at 25 °C.

ficient than by the protiated alcohol in each case, but was found to follow similar dependences on concentration. Figure 3a shows representative plots of  $k_{\text{decay}}$  versus  $[\text{MeOL}]$  ( $\text{L} = \text{H}$  or  $\text{D}$ ) for **5d** and **5f** in acetonitrile solution at 25 °C. Fitting of the data for **5g** to eq 3 afforded values for the second-order rate constants ( $k_{\text{MeOL}}$ ;  $\text{L} = \text{H}$  or  $\text{D}$ ) that were equal to zero within experimental error; as expected, a plot of  $k_{\text{decay}}$  versus  $[\text{MeOL}]^2$  was linear for this silene, as illustrated in Figure 3b. An upper limit of ca.  $2 \times 10^4 \text{ M}^{-1} \text{ s}^{-1}$  is

estimated for the second-order rate coefficients ( $k_{\text{MeOL}}$ ) in these cases.

$$k_{\text{decay}} = k_0 + k_{\text{MeOH}}[\text{MeOH}] + k_{2\text{MeOH}}[\text{MeOH}]^2 \quad (3)$$

Table 2 lists the second- and third-order rate constants determined in these experiments for reaction of **5c–g** with MeOH, AcOH, and *n*-BuNH<sub>2</sub> in acetonitrile solution at 25 °C. The rate constants for reaction with MeOD and AcOD are not listed as such, but rather as  $k_{\text{H}}/k_{\text{D}}$  values calculated from the corresponding data for the protiated and deuterated reagents. For comparison, the table also includes values previously reported rate constants for reaction of **5a,b** with the same three reagents under similar conditions.<sup>11,14</sup>

## Discussion

As expected,<sup>15</sup> photolysis of **6c–g** in solution affords the corresponding silenes **5c–g** in high chemical yields in every case, as indicated by the formation of the methoxysilanes **7c–g** upon photolysis of the five silacyclobutanes in methanolic hexane solution. We were somewhat surprised to find that in all five cases isomers of the silacyclobutanes are also formed in significant yields. These products invariably exhibit GC retention times and mass spectra that are very similar to those of the starting silacyclobutane, which led us to suspect they might be the products of phototransposition of (one of) the *ortho*-methyl-substituted aryl rings in **6c–g**. This suspicion was confirmed with the identification of **8c** as the product in question from photolysis of **6c**. The formation of such products is well-known in the photochemistry of benzene derivatives,<sup>13</sup> and it has been observed previously upon photolysis of a tetrasilyl-substituted benzene in solution.<sup>16</sup> However, to our knowledge it has not been observed previously from arylsilacyclobutanes, including the various *para*-substituted 1,1-diaryl derivatives that we have studied.<sup>11,17</sup> This means either that the chemistry responsible for the process is much more efficient in *ortho*-methylphenyl-substituted systems than in *para*-methylphenyl systems or that it occurs in both *ortho*- and *para*-

(14) Leigh, W. J.; Li, X. *J. Phys. Chem. A* **2003**, *107*, 1517.

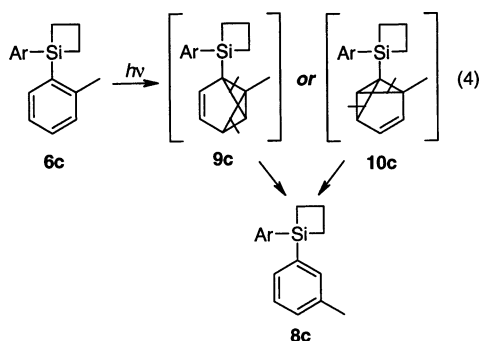
(15) Steinmetz, M. G. *Chem. Rev.* **1995**, *95*, 1527.

(16) West, R.; Furue, M.; Rao, V. N. M. *Tetrahedron Lett.* **1973**, 911.

(17) Leigh, W. J.; Li, X. *J. Am. Chem. Soc.* **2003**, *125*, 8096.

substituted systems but leads to an identity reaction in the case of the latter, and is hence undetectable. We favor the former explanation on the basis of the laser flash photolysis results for **6b–g**, which demonstrate that those derivatives that afford the corresponding rearrangement products in highest yields (**6c–f**) also show the highest apparent yields of the second, shorter-lived transient species. We suspect, but cannot yet confirm (*vide infra*), that these transients are related to the phototransposition chemistry, as we have not observed behavior of this type in any of the arylsilylcyclobutane derivatives whose photochemistry we have studied previously.<sup>11,17–19</sup>

The phototransposition of substituted benzene derivatives is thought to proceed via excited singlet state isomerization to a benzvalene derivative, which is then transformed into the aromatic isomer via triplet-sensitized (quantum chain) decomposition.<sup>13</sup> In the case of **6c**, as with any unsymmetrically disubstituted benzene derivative, the initial isomerization can in principle lead to six distinct benzvalene isomers, of which two (**9c** and **10c** in eq 4) would yield **8c** upon triplet-sensitized decomposition; the other four leave the *ortho*-substituent unchanged from its initial position. Unfortunately, we are unable to identify the specific regioisomer involved in the rearrangement on the basis of the results we have.



Laser flash photolysis of **6c–g** allows the detection of the corresponding silenes **5c–g**, which can be identified on the basis of their UV absorption maxima and characteristic reactivity toward nucleophiles. In all cases but **6g**, laser photolysis also affords a second, shorter-lived transient product that we have not been able to identify because their lifetimes are unresponsive to the addition of reagents that are known to quench triplet states (i.e., oxygen), silicon–carbon multiple bonds and silylenes (i.e., MeOH), silyl radicals (i.e., chloroform), or radical cations (i.e., triethylamine). Experiments with samples of **6c–f** of exceptionally high (>99.5%) purity verified that these transients are not impurity-related. Furthermore, their absorption spectra and lifetimes are not what might be expected for the benzvalene isomers that the steady state photolysis experiments suggest are also formed in the photolyses of these compounds. Nevertheless, we suspect that they are related to the phototransposition chemistry, since analogous transients are not formed from any of the *para*-substituted 1,1-diarylsilylcyclobutanes that we have

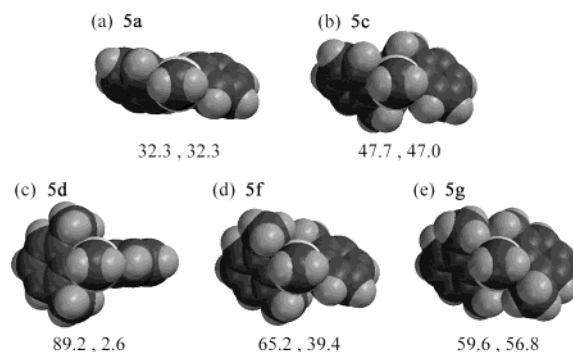
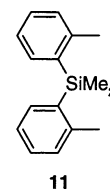


**Figure 4.** Calculated (HF/3-21G\*\*/HF/3-21G\*) structures of *ortho*-methyl-substituted 1,1-diarylsilenes **5c** (a), **5d** (b), **5f** (c), and **5g** (d), viewed along the Si=C bond axes. Each structure is labeled with the calculated angles that the planes of the two aryl rings make with respect to the plane of the Si=C bond.

studied previously. While we are unaware of any corroborating evidence for this assignment in the literature, we note that a transient species with properties similar to those observed in the present work is also formed upon (248 nm) laser irradiation of the related acyclic arylsilane **11**.<sup>20</sup>



The UV absorption spectra of the silenes **5c–g** exhibit significant hypsochromic shifts compared to those of **5a** and **5b** ( $\lambda_{\max} = 325$  nm in hexane and MeCN at 25 °C<sup>11</sup>), with the magnitude of the effect increasing as the number of *ortho*-methyl substituents increases. The effect is particularly pronounced in the case of **5g** ( $\lambda_{\max} = 295$  nm) and is consistent with decreased conjugation of the aryl ring(s) with the Si=C bond as the number of *ortho*-methyl substituents is increased. The trend is borne out by the calculated (RHF/3-21G\*) structures of **5a**, **5c**, **5d**, **5f**, and **5g**, which are shown in space-filling format in Figure 4; the structures are arranged with the viewing axis coincident with the Si=C bonds in the five molecules and are labeled with the dihedral angles that define the twist angles between the planes of the two aryl rings and the plane of the Si=C bond. The calculated Si=C bond lengths in the five structures are all equal to  $1.69 \pm 0.005$  Å, in good agreement with the values calculated previously for other, simpler silenes at the same or higher levels of theory.<sup>21–24</sup>

Accompanying the gradual blue-shift in absorption maximum with increasing steric hindrance is a pronounced increase in the lifetimes ( $1/k_0$ ) of **5c–g** throughout the series. In scrupulously dry solution, silenes are expected to exhibit second-order decay kinetics due to

(20) Owens, T. R.; Leigh, W. J. Unpublished.

(21) Apeloig, Y.; Karni, M. *J. Am. Chem. Soc.* **1984**, *106*, 6676.

(22) Nagase, S.; Kudo, T.; Ito, K. In *Applied Quantum Chemistry*; Smith, V. H., Jr., Schaefer, H. F., Morokuma, K., Eds.; D. Reidel: Dordrecht, 1986; pp 249–267.

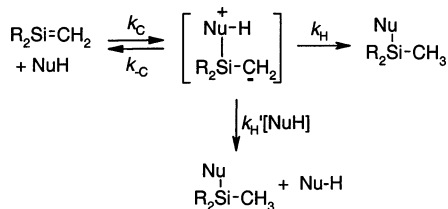
(23) Seidl, E. T.; Grev, R. S.; Schaefer, H. F., III. *J. Am. Chem. Soc.* **1992**, *114*, 3643.

(24) Veszpremi, T.; Takahashi, M.; Hajgato, B.; Kira, M. *J. Am. Chem. Soc.* **2001**, *123*, 6629.

(18) Leigh, W. J.; Boukherroub, R.; Bradaric, C. J.; Cserti, C. C.; Schmeisser, J. M. *Can. J. Chem.* **1999**, *77*, 1136.

(19) Leigh, W. J.; Owens, T. R. *Can. J. Chem.* **2000**, *78*, 1459.

Scheme 1



dimerization,<sup>1</sup> a process that proceeds in head-to-tail fashion to yield the corresponding 1,3-disilacyclobutane in the case of **5a**.<sup>25–27</sup> In the present cases however, the silene absorptions appeared to decay with reasonably clean (pseudo-) first-order kinetics in both solvents examined, a feature that is usually due to reaction with trace amounts of impurities (e.g., water) in the solvent. We have been unable to obtain any evidence from steady state photolysis experiments for the formation of either silene dimers or the disiloxanes expected from reaction with adventitious water, so we are uncertain as to how to interpret the silene lifetimes in the absence of intentionally added reagents. Nevertheless, whatever reaction is responsible for the decay of the silenes in the pure, dry solvents employed in this work, our results indicate clearly that its rate constant decreases substantially with increasing *ortho*-methyl substitution throughout the series.

Exactly the same trend is observed in the absolute rate constants for reaction of **5c–g** with *n*-butylamine, acetic acid, and methanol (Table 2). These reactions are all thought to begin with attack of the neutral nucleophile (NuH) at the silenic silicon atom, to yield a zwitterionic addition complex which proceeds to product by proton transfer to the silenic carbon.<sup>1</sup> In general, the latter can proceed via two mechanisms: an uncatalyzed pathway in which proton transfer occurs unimolecularly within the zwitterionic complex, and a catalytic pathway in which proton transfer is assisted by a second molecule of the nucleophile, acting as either an acid or base. The general mechanism is shown in Scheme 1. In the case of alcohol additions, Kira and co-workers have demonstrated that the intracomplex proton pathway proceeds with *syn* stereochemistry, while the catalytic pathway proceeds with *anti* stereochemistry, most likely via a protonation–deprotonation sequence.<sup>28</sup> In any event, application of the steady state approximation for the zwitterionic intermediate leads to the expression shown in eq 5 for the rate constant for decay of the silene ( $k_{\text{decay}}$ ) in the presence of NuH, which transforms to the quadratic eq 6 over the (low to intermediate) concentration range where  $(k_{-C} + k_H) \gg k_H'[\text{NuH}]$ . The scheme predicts that  $k_{\text{decay}}$  should follow a linear dependence on  $[\text{NuH}]$  in the limiting situation where  $k_H \gg k_H'[\text{NuH}]$ , a linear dependence on  $[\text{NuH}]^2$  in the limit where  $k_H \ll k_H'[\text{NuH}]$ , and a quadratic dependence on  $[\text{NuH}]$  in situations in between.

$$k_{\text{decay}} = k_0 + \frac{k_C[\text{NuH}]}{\{k_{-C} + k_H + k_H'[\text{NuH}]\}} \{k_H + k_H'[\text{NuH}]\} \quad (5)$$

$$k_{\text{decay}} = k_0 + \frac{k_C[\text{NuH}]}{(k_{-C} + k_H)} \{k_H + k_H'[\text{NuH}]\} \quad (6)$$

The additions of *n*-butylamine and acetic acid both exhibit linear dependences of  $k_{\text{decay}}$  on  $[\text{NuH}]$  concentration, as they do with all other silenes that have been studied to date.<sup>1</sup> For *n*-butylamine addition, the linear behavior is most reasonably accounted for by the first of the three kinetic conditions described above; that is, it results from the intracomplex proton transfer pathway being significantly faster than the extracomplex pathway ( $k_H \gg k_H'[\text{NuH}]$ ) over the ranges of amine concentration that can be examined.<sup>14,29</sup> While isotope effect data have not been obtained for this reaction, the temperature dependence of the rate constants for addition of *n*-BuNH<sub>2</sub> to **5a** is strongly nonlinear, consistent with the proton transfer step being the rate-determining step for reaction.<sup>14</sup> In the case of acetic acid, on the other hand, the linear dependence of  $k_{\text{decay}}$  on  $[\text{NuH}]$  most likely results from the relatively high acidity of the reagent, which increases the rate constant for proton transfer to the extent that  $k_H \gg k_{-C}$  in Scheme 1 and the initial complexation step is the rate-determining step for reaction. As this explanation demands, no deuterium kinetic isotope effect is observed on the bimolecular rate constants for reaction of **5c–g** or any of the other 1,1-diarylsilenes that we have studied previously, and the activation energy for reaction of AcOH with **5a** is positive.<sup>11</sup> In fact, the lack of a KIE on the addition of AcOH to **5g**, for which  $k_{\text{AcOH}} \approx 4 \times 10^6 \text{ M}^{-1} \text{ s}^{-1}$  (see Table 2), provides the strongest evidence obtained to date that the addition of this reagent must follow the mechanism of Scheme 1 rather than via a concerted mechanism or one involving initial protonation of the Si=C bond. In the case of **5a**, the absence of a KIE on  $k_{\text{AcOH}}$ <sup>11</sup> is not particularly compelling evidence for one mechanism or the other since the rate constant for the reaction is within a factor of ca. 10 of the diffusion-controlled rate, and a primary KIE would hence be expected to be small and difficult to detect by our methods. Additional evidence that the mechanisms for addition of *n*-BuNH<sub>2</sub> and AcOH are effectively identical is provided by the similar trends in the rate constants observed for reaction of **5a–g** with the two reagents; there can be little question that amine addition to the Si=C bond in these molecules must begin with nucleophilic attack at silicon.

Methanol addition exhibits a functional dependence of  $k_{\text{decay}}$  on  $[\text{NuH}]$  that varies consistently throughout the series, from linear in the cases of **5a–c** (i.e.,  $k_H \gg k_H'[\text{NuH}]$ ), through quadratic in the cases of **5d–f** (i.e.,  $k_H \approx k_H'[\text{NuH}]$ ), to a purely squared dependence in the case of **5g** (i.e.,  $k_H \ll k_H'[\text{NuH}]$ ). Thus, in this case there is clear evidence for a change in reaction mechanism with increasing steric bulk of the substituents attached to silicon. The change from linear to quadratic behavior in the kinetics of alcohol addition is normally associated with a reduction in the electrophilicity of the Si=C bond due to the *electronic* effects of substituents.<sup>1</sup> A situation in which it is reduced so dramatically that a second-

(25) Auner, N.; Grobe, J. *J. Organomet. Chem.* **1980**, *197*, 147.

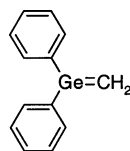
(26) Jutzi, P.; Langer, P. *J. Organomet. Chem.* **1980**, *202*, 401.

(27) Toltl, N. P.; Stradiotto, M. J.; Morkin, T. L.; Leigh, W. J. *Organometallics* **1999**, *18*, 5643.

(28) Kira, M.; Maruyama, T.; Sakurai, H. *J. Am. Chem. Soc.* **1991**, *113*, 3986.

(29) The highest quencher concentration employable is defined by the quenching rate constant and the shortest lifetimes that can be measured reliably by our system (ca. 50 ns).

order kinetic component cannot be detected at all has never been observed previously in silenes, although it is interesting to note that this is exactly the behavior exhibited by the reaction of methanol with the intrinsically less electrophilic Ge=C bond of 1,1-diphenylgermene (**12**).<sup>30</sup>



12

The second-order rate constants for all three reactions exhibit similar trends with increasing numbers of *ortho*-methyl groups in **5c–g**, with those for methanol addition being the most sensitive. This is clearly the result expected if the three reagents react via the same reaction mechanism. Comparison of the rate constants for addition of the three nucleophiles to **5c** with the corresponding values for addition to **5a** and/or **5b** indicates that a *single ortho*-methyl substituent on each of the aryl rings has little or no effect—either steric or electronic—on the reaction kinetics. According to the calculated structure of **5c** (Figure 4b), the aryl rings are twisted ca. 47° out of the plane of the Si=C bond, which can be compared to the corresponding twist angle of 32° predicted for **5a** at the same level of theory. Presumably, the twist angle in **5c** is not severe enough for the *ortho*-methyl groups to significantly shield either face of the Si=C bond from nucleophilic attack, and so the second-order rate constants for reaction of this compound are similar to those for the parent molecule. As comparison of the data for **5c** and **5d** reveals, the situation is quite different when the two *ortho*-methyl groups are placed on the same ring, resulting in a 15- to 30-fold rate reduction in the cases of amine and acetic acid addition and a ca. 400-fold rate reduction for methanol addition. The calculated lowest energy conformation of **5d** (Figure 4c) indicates that, as expected, the 2,6-dimethylphenyl substituent is approximately perpendicular to the plane of the Si=C bond, while the phenyl ring is nearly coplanar to it; a substantial rate reduction results from the fact that both faces of the Si=C bond are now “half-blocked” compared to the situation in **5a** and **5c**. Placing a third *ortho*-methyl group in the molecule, as in **5f** (Figure 4d), causes less than a 3-fold reduction in the second-order rate constant for addition of the three reagents compared to **5d** or the mesityl-substituted silene **5e**, which contains an equal total number of methyl groups on the aryl rings. Presumably, the rate reductions are relatively small because one face of the Si=C bond remains “half-blocked”; that is, it retains steric shielding similar to that characterizing the two faces of the Si=C bond in **5d**, and because the proton transfer step proceeds with *syn* stereochemistry, both steps of the reaction proceed on the same face. Finally, substitution with the fourth *ortho*-methyl group, as in **5g**, results in a further 10-fold reduction in reactivity. The very small differences between the rate constants for reaction of **5d** and **5e** with each of the three reagents suggest strongly that this effect is almost entirely steric

in origin; the calculated structure of **5g** (Figure 4e) suggests that it is due to both faces of the Si=C bond being “fully blocked”. In the case of methanol addition, this reduces the second-order rate constant to  $<2 \times 10^4 \text{ M}^{-1} \text{ s}^{-1}$ , a value small enough that the second-order reaction pathway no longer competes effectively with the third-order (catalytic) pathway, even at methanol concentrations as low as ca. 10 mM.

The gradual change in mechanism for methanol addition to **5c–g** as steric effects increase suggests that the effect on the kinetics originates primarily in the structures of the zwitterionic addition complexes that result from initial attack of the neutral nucleophile at the silenic silicon. Increased steric shielding can be expected to force a lengthening of the weak Si–Nu bond in the complex and, with it, a reduction in the degree of charge transfer from the nucleophilic site to the silenic carbon. This reduces both the acidity of the proton and the basicity of the silenic carbon in the complex, which in turn leads to a reduction in the rate of internal proton transfer.

The third-order rate constants for addition of MeOH to **5d–g** vary over 2 orders of magnitude, but show one interesting difference compared to the second-order rate constants for reaction of this nucleophile; whereas the second-order rate constant for reaction of **5f** is identical to that of **5e**, the third-order rate constants differ by a factor of ca. 6. This is consistent with the mechanism of Kira and co-workers, who proposed that reaction by this pathway proceeds via *anti*-protonation of the silenic carbon in the zwitterionic complex by a second molecule of alcohol.<sup>28</sup> Formation of the zwitterionic complexes of **5e** and **5f** can proceed in both cases via attack of methanol at a half-blocked face of the Si=C bond; thus, the overall second-order rate constants are similar for the two compounds because intracomplex proton transfer must occur in *syn* fashion. For the third-order process, protonation must occur at the face of the Si=C bond opposite that bonded to the nucleophile, which is also a half-blocked face in the case of **5e**. In **5f**, however, protonation must occur at the fully blocked face, and hence the overall rate constant is reduced.

## Summary and Conclusions

The effects of *ortho*-methyl substitution on the kinetics and mechanisms of the [1,2]-addition of alcohols, primary amines, and carboxylic acids to the Si=C bonds of transient 1,1-diarylsilenes have been systematically assessed.

1,1-Bis(2-methylphenyl)silene (**5c**) exhibits a lifetime, UV absorption maximum, and reactivity in solution similar to those of its di(*para*-methyl)-substituted isomer (**5b**), indicating that the electronic effect of the *ortho*-methyl group on Si=C bond electrophilicity is small and similar to that resulting from *para*-methyl substitution. On the other hand, methyl substitution at both *ortho*-carbons of one or both of the aryl rings in **5** results in progressive reductions in reactivity, as measured by the lifetime in the absence of silene traps and the absolute rate constants for reaction with nucleophiles. The effects are ascribable to steric protection at silicon, the initial reaction site in the two-step mechanism for nucleophilic addition. The most highly hindered silene studied in this work, 1,1-bis(2,6-dimethylphenyl)-

(30) Tolft, N. P.; Leigh, W. J. *J. Am. Chem. Soc.* **1998**, *120*, 1172.

silene (**5g**), exhibits a lifetime of 6–8 ms, which should be compared to that of 1-(2,6-dimethylphenyl)-1-phenylsilene (**5d**;  $\tau^{\text{MeCN}} \approx 140 \mu\text{s}$ ) and 1,1-bis(2-methylphenyl)silene (**5c**;  $\tau^{\text{MeCN}} \approx 8 \mu\text{s}$ ). Similarly, the absolute second-order rate constant for reaction of **5g** with methanol is at least 40 times slower than that of **5d** and at least 10 000 times slower than that of **5c**. The overall mechanism of the reaction also changes throughout the series, from one that is purely first-order in alcohol over the concentration range studied in the case of **5c** to one that is purely second-order in alcohol in the case of **5g**; reaction via both pathways is kinetically observable in the moderately hindered derivatives in the series. Detailed analysis of the rate constants provides support for previous suggestions by Kira and co-workers<sup>28</sup> that the second-order pathway involves catalytic proton transfer within the initially formed silene-alcohol complex via a protonation–deprotonation sequence.

Similar trends in reactivity are observed for the addition of *n*-butylamine and acetic acid, but they span a somewhat smaller range because of the higher intrinsic reactivity of these nucleophiles in silene [1,2]-addition reactions, and both exhibit a clean first-order dependence on nucleophile concentration for all silenes in the series. Nevertheless, the similarities are consistent with a common, two-step mechanism for the addition of the three types of nucleophiles to the Si=C bond in **5**, initiated by attack of the neutral nucleophile at the silenic silicon atom.

### Experimental Section

Details of the synthesis and characterization of compounds are available as Supporting Information.

Nanosecond laser flash photolysis experiments employed the pulses (248 nm; 15–20 ns; 70–120 mJ) from a Lambda Physik Compex 100 excimer laser, filled with F<sub>2</sub>/Kr/He mixtures, and a Luzchem Research mLFP-111 laser flash photolysis system. The latter was modified to incorporate an external 150 W high-pressure Xe lamp as monitoring source, powered by a Kratos LPS-251HR power supply. Solutions were prepared at concentrations such that the absorbance at the excitation wavelength (248 nm) was ca. 0.7 (ca. 0.002 M) and were flowed continuously through a thermostated 7 × 7 Suprasil flow cell connected to a calibrated 100 mL reservoir. Solution temperatures were measured with a Teflon-coated copper/constantan thermocouple that was inserted directly into the flow cell. Reagents were added directly to the reservoir by microliter syringe as aliquots of standard solutions. Rate constants were calculated by linear or polynomial least-squares analysis of decay rate-concentration data (6–15 points) that spanned at least a factor of 5 (usually more than 1 order of magnitude) in the transient decay rate (see eqs 2 and 3). Errors are quoted as twice the standard deviation obtained from the least-squares analysis.

**Acknowledgment.** We thank the McMaster Regional Centre for Mass Spectrometry for mass spectrometric analyses, and the Natural Sciences and Engineering Research Council of Canada for financial support.

**Supporting Information Available:** Transient absorption spectra of **5e** and **5f**, and details of the synthesis and characterization of compounds and photoproducts. This material is available free of charge via the Internet at <http://pubs.acs.org>.

OM030594P